

# Meiosis-Induced Double-Strand Break Sites Determined by Yeast Chromatin Structure

Tzu-Chen Wu and Michael Lichten\*

Double-strand DNA breaks (DSBs) occur at recombination hotspots during *Saccharomyces cerevisiae* meiosis and are thought to initiate exchange at these loci. Analysis of DSB sites in three regions of the yeast genome indicated that breaks occur at or near many potential transcription promoters and that DSBs initiate most, if not all, meiotic recombination. DSB sites displayed deoxyribonuclease I hypersensitivity in chromatin from mitotic and meiotic cells, and changes in chromatin structure produced parallel changes in the occurrence of DSBs. Thus, features of chromatin structure that are established before meiosis play a role in determining where meiotic recombination events initiate.

Transient DSBs occur early in meiosis I prophase in the yeast *Saccharomyces cerevisiae* at loci that display elevated frequencies of meiotic gene conversion and crossing-over (1–4). Deletions and other rearrangements at these hotspots lead to parallel changes in both DSB and recombination frequencies (5–7). DSBs are not seen in DNA from mitotic cells and appear during meiosis at the time of commitment to meiotic recombination (1, 4, 8). Repair of these meiosis-induced breaks is accompanied by chromosome synapsis and the production of physically recombined DNA molecules (2, 4, 8, 9). In wild-type cells, DSB ends are recised to produce DNA molecules with 3' single-stranded overhangs (10), consistent with the strand polarity observed in heteroduplex DNA in spores (11). Meiotic recombination is absent both in mutants that block DSB formation (2, 6, 12) and in *rad50*s mutants, in which breaks are formed but are not recised or repaired (2, 10). DSBs are also formed in mutants with an inactive *DMC1* gene (*DMC1* encodes a meiosis-induced *recA* homolog); in these cells, breaks are not repaired and undergo extensive 5' to 3' resection, producing DNA molecules with 3' single-stranded overhangs that are much longer than those observed in wild-type cells (13). Thus, both temporal and mutant analyses indicate that meiotic exchange at recombination hotspots is initiated by the *in vivo* formation and repair of DSBs.

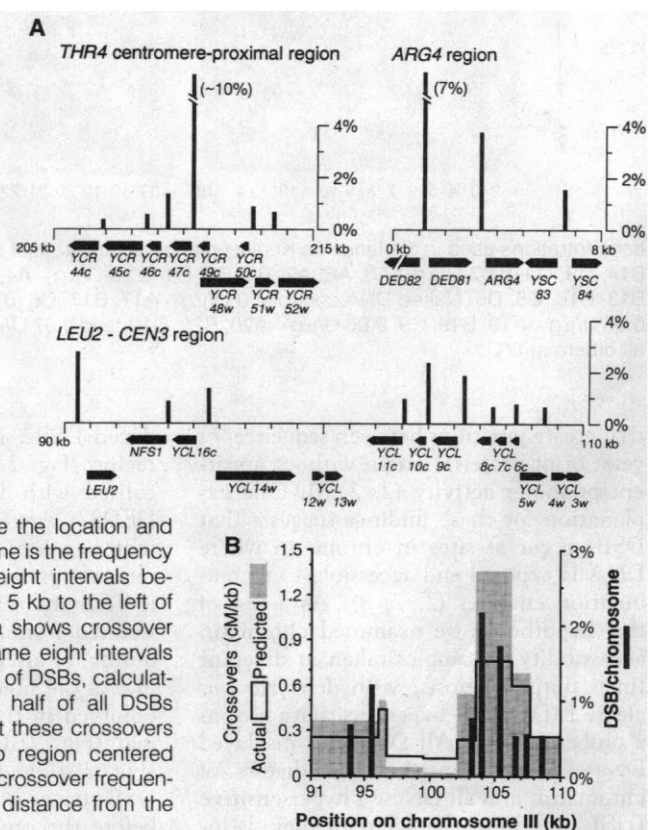
DSBs also occur in regions of the *S. cerevisiae* genome that display low to moderate recombination frequencies (14). The factors that determine where DSBs occur, both at hotspots and in other regions of the genome, remain to be fully established. To address this issue, we analyzed meiosis-induced DSBs in three regions

that collectively comprise ~38 kb of yeast genomic sequences (Fig. 1A). We chose two of these regions (*ARG4* and *THR4* centromere-proximal) because they contain meiotic recombination hotspots (3). The third region, *LEU2-CEN3*, was chosen because it displays a frequency of crossovers [0.3 centimorgan (cM)] per kilobase of DNA that is similar to the average estimated for the entire yeast genome (15) and because a fine-structure map of meiotic crossovers in this region has been determined (16). As expected, the three sites with the greatest break frequencies were at previously identified recombination hotspots (1, 3); in addition, 15 other sites displayed detectable

DSBs (>0.3% of a single copy sequence). All 18 DSB sites were located adjacent to the 5' end of an open reading frame, in a potential promoter region, and DSBs occurred in the majority (18 of 23) of promoter regions identified by this criterion (Fig. 1A). We compared the distributions of DSBs and of meiotic crossovers in the *LEU2-CEN3* region. The frequency of DSBs in this region (8% of chromosomes) is sufficient to account for all of the meiotic crossovers that occur (6 cM), and the distribution of DSBs (Fig. 1B) is similar to the distribution of meiotic crossovers. If the meiotic behavior of the *LEU2-CEN3* region is representative of the yeast genome as a whole, then these results indicate that most, if not all, meiotic recombination is initiated by promoter-associated DSBs.

Although the close correspondence between DSB sites and potential promoters might suggest a direct causal relation between active transcription and meiotic recombination, several observations are inconsistent with this hypothesis. Certain promoter mutations in the *ARG4* and *HIS4* markedly reduce transcription without affecting hotspot activity (17); conversely, translocation of *ARG4* to other chromosomal locations can eliminate DSBs in the *ARG4* promoter without abolishing transcription (8). In addition, DSBs often occur in artificial constructs

**Fig. 1.** Location and frequency of DSBs. (A) DSB frequencies and locations in the three regions examined. Bar heights indicate the fraction of chromosomes suffering DSBs at each site (26). Horizontal arrows indicate open reading frames predicted by DNA sequence (21, 27). Horizontal coordinates and gene names for the *THR4* centromere-proximal and *LEU2-CEN3* regions are from the nucleotide sequence of chromosome III (21); coordinates in the *ARG4* region are arbitrary. (B) Crossover and DSB distributions in the *LEU2-CEN3* region. Vertical black bars are the location and frequency of DSBs. The solid line is the frequency of crossing-over (cM/kb) in eight intervals between *LEU2* and an *Mlu* I site 5 kb to the left of *CEN3* (28). The shaded area shows crossover frequencies (cM/kb) in the same eight intervals predicted from the distribution of DSBs, calculated with the assumption that half of all DSBs produced crossovers and that these crossovers were distributed over a 3-kb region centered around the DSB site, with the crossover frequencies decreasing linearly with distance from the DSB site.



Laboratory of Biochemistry, Division of Cancer Biology, Diagnosis and Centers, National Cancer Institute, National Institutes of Health, Building 37, Room 4D14, Bethesda, MD 20892.

\*To whom correspondence should be addressed.

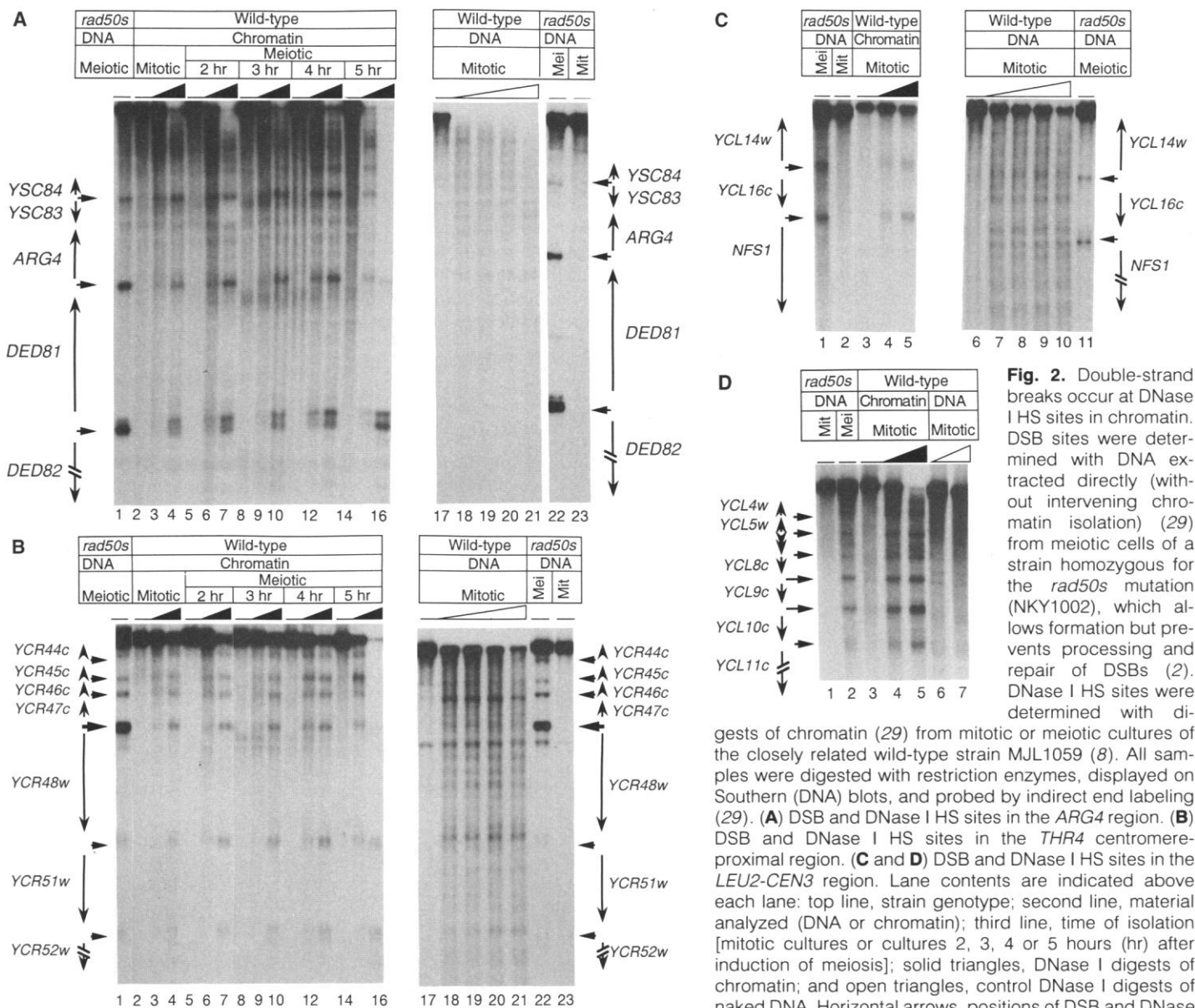


**Fig. 2.** Double-strand breaks occur at DNase I HS sites in chromatin. DSB sites were determined directly (without intervening chromatin isolation) (29) from meiotic cells of a strain homozygous for the *rad50s* mutation (NKY1002), which allows formation but prevents processing and repair of DSBs (2). DNase I HS sites were determined with digests of chromatin (29) from mitotic or meiotic cultures of the closely related wild-type strain MJL1059 (8). All samples were digested with restriction enzymes, displayed on Southern (DNA) blots, and probed by indirect end labeling (29). (A) DSB and DNase I HS sites in the *ARG4* region. (B) DSB and DNase I HS sites in the *THR4* centromere-proximal region. (C and D) DSB and DNase I HS sites in the *LEU2-CEN3* region. Lane contents are indicated above each lane: top line, strain genotype; second line, material analyzed (DNA or chromatin); third line, time of isolation [mitotic cultures or cultures 2, 3, 4 or 5 hours (hr) after induction of meiosis]; solid triangles, DNase I digests of chromatin; and open triangles, control DNase I digests of naked DNA. Horizontal arrows, positions of DSB and DNase I HS sites; vertical arrows, open reading frames. DNase

concentrations used in the lanes (in Kunitz units per microgram of DNA) are as follows: chromatin: 0 U/ $\mu$ g—A2, A5, A8, A11, A14, B2, B5, B8, B11, B14, C3, D3; 0.07 U/ $\mu$ g—A3, A6, A9, B3, B6, B9; 0.13 U/ $\mu$ g—A4, A7, A10, A12, A15, B4, B7, B10, B12, B15, C4, D4; and 0.3 U/ $\mu$ g—A13, A16, B13, B16, C5, D5. Naked DNA controls: 0 U/ $\mu$ g—A17, B17, C6; 0.0003 U/ $\mu$ g—D6; 0.0007 U/ $\mu$ g—D7; 0.04 U/ $\mu$ g—C7; 0.45 U/ $\mu$ g—A18, B18, C8; 0.05 U/ $\mu$ g—A19, B19, C9; 0.06 U/ $\mu$ g—A20, B20, C10; and 0.07 U/ $\mu$ g—A21, B21. Samples in lanes D6 and D7 were digested with DNase I at 37°C; all others at 0°C.

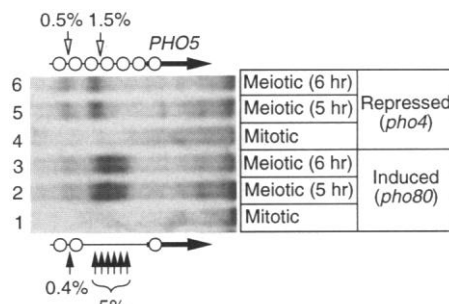
that create junctions between sequences of yeast or of bacterial origin without apparent promoter activity (2, 7, 8). One explanation for these findings suggests that DSBs occur at sites in chromatin where DNA is exposed and accessible to recombination enzymes (2, 7, 8). As a test of this hypothesis, we examined chromatin accessibility in samples taken at different times during meiosis, with deoxyribonuclease I (DNase I) hypersensitivity (18) as a probe (Fig. 2). All DSB sites displayed DNase I hypersensitivity in digests of chromatin, and all DNase I hypersensitive (HS) sites were the locus of meiosis-in-

duced DSBs. For example, in the *ARG4* region (Fig. 2A), DNase I HS sites colocalized with DSB sites in the *DED81/DED82*, *ARG4*, and *YSC83/YSC84* promoter regions. This hypersensitivity pattern was present in chromatin from mitotic cells and was unchanged in chromatin isolated from meiotic cell either before, during, or after the time of DSB formation [ $3.6 \pm 0.4$  hours (8)]. Similar results were observed in the *THR4* centromere-proximal (Fig. 2B) and *LEU2-CEN3* regions (Fig. 2, C and D). The observation that DSBs occur at DNase I HS sites present before the onset of meiosis makes it un-

likely that DSB formation involves a meiosis-induced remodeling of chromatin. Instead, these data indicate that DSBs are formed by a system that acts at preexisting exposed sites in chromatin.

To further test the relation between chromatin structure and DSBs we determined the effect that altering chromatin structure had on the pattern of DSBs in sequences upstream of the *PHO5* gene, which encodes an inducible acid phosphatase. Positioned nucleosomes occlude much of the region upstream of *PHO5* when the gene is repressed; induction is accompanied by a transcription-indepen-

**Fig. 3.** Altering chromatin structure in the *PHO5* promoter region leads to a parallel change in DSBs. DNA was extracted without intervening chromatin isolation from mitotic or meiotic cultures [5 or 6 hours (hr) after induction of meiosis] of *pho4* or *pho80* derivatives of the *rad50s* strain NKY1002. Samples were displayed on Southern blots and probed by indirect end labeling to detect DSBs in the *PHO5* promoter region (30). As described in the text, in *pho4* cells, positioned nucleosomes occupy the entire *PHO5* promoter region; in *pho80* cells, four of these nucleosomes are disrupted. Previously determined locations of positioned nucleosomes (19), indicated by circles, are shown at the top (*pho4*) and bottom (*pho80*) of the figure relative to *PHO5* coding sequences (horizontal arrows), along with the position and frequency of DSBs (open vertical arrows, *pho4*; solid vertical arrows, *pho80*).



dent disruption of four of these nucleosomes to create a large open region (19). This chromatin remodeling is accompanied by a parallel change in the distribution of DSBs (Fig. 3). In *pho4* mutant cells, where *PHO5* is repressed (20), DSBs occurred at low frequencies at two sites located about 850 and 550 nucleotides (nts) upstream of the start of *PHO5* translation. In *pho80* mutant cells, where *PHO5* is induced (20), the frequency of DSBs in the *PHO5* promoter increased markedly, and most DSBs were distributed over a 450-nt interval (-600 to -150) in the region of induction-associated nucleosome disruption.

In summary, our results are consistent with the suggestion that meiotic recombination is initiated by DSBs both at hotspots and in other regions of the yeast genome; these breaks form primarily in intergenic regions that contain transcription promoters. The promoters of several yeast genes have been shown to be more exposed than the bulk of chromatin (18). Our results may indicate that most, if not all, yeast promoters share this property, presumably to allow access by components of the transcription machinery. We suggest that, as a consequence, sequences in and around the promoters of most yeast genes are also more accessible to enzymes that form DSBs during meiosis and thus serve as preferential sites for the initiation of recombination. This suggestion is supported by the observed correlation between patterns of gene density and genetic recombination along chromosome III (21) and by the fact that all naturally occurring meiotic recombination hotspots in *S. cerevisiae* characterized to date are located in promoter regions (3, 17). The frequency of DSBs at a site may well be affected by other factors, such as recognition of bound proteins, features of DNA structure, or competition with other nearby DSB sites; nevertheless, we expect that openness of chromatin will be a primary determinant of whether recombination is initiated at a particular site.

Control of target site accessibility has also been suggested to account for the unidirectional nature of gene conversion in yeast mating-type switching (22) and to explain switch-site activation during immunoglobulin gene rearrangement (23). Our results may also provide an explanation for the known differences in genetic maps derived from male and female meioses in humans and mice (24). In both organisms, certain regions undergo recombination more frequently during spermatogenesis than during oogenesis, and vice versa; these may result from differences in chromatin structure (and thus accessibility to recombination enzymes) that accompany sex-specific patterns of gene expression during gametogenesis.

REFERENCES AND NOTES

1. H. Sun, D. Treco, N. P. Schultes, J. W. Szostak, *Nature* **338**, 87 (1989).
2. L. Cao, E. Alani, N. Kleckner, *Cell* **61**, 1089 (1990).
3. A. Nicolas, D. Treco, N. P. Schultes, J. W. Szostak, *Nature* **338**, 35 (1989); N. P. Schultes and J. W. Szostak, *Genetics* **126**, 813 (1990); M. Goldway, A. Sherman, D. Zenvirth, T. Arbel, G. Simchen, *ibid.* **133**, 159 (1993).
4. D. K. Nag and T. D. Petes, *Mol. Cell. Biol.* **13**, 2324 (1993).
5. V. Rocco, B. de Massy, A. Nicolas, *Proc. Natl. Acad. Sci. U.S.A.* **89**, 12068 (1992).
6. R. E. Malone, personal communication.
7. B. de Massy and A. Nicolas, *EMBO J.* **12**, 1459 (1993); T.-C. Wu, C. Goyon, M. Lichten, unpublished data.
8. C. Goyon and M. Lichten, *Mol. Cell. Biol.* **13**, 373 (1993).
9. R. Padmore, L. Cao, N. Kleckner, *Cell* **66**, 1239 (1991).
10. H. Sun, D. Treco, J. W. Szostak, *ibid.* **64**, 1155 (1991).
11. M. Lichten *et al.*, *Proc. Natl. Acad. Sci. U.S.A.* **87**, 7653 (1990); D. K. Nag and T. D. Petes, *Genetics* **125**, 753 (1990).
12. E. Alani, R. Padmore, N. Kleckner, *Cell* **61**, 419 (1990).
13. D. K. Bishop, D. Park, L. Xu, N. Kleckner, *ibid.* **69**, 439 (1992).
14. D. Zenvirth *et al.*, *EMBO J.* **11**, 3441 (1992); J. C. Game, *Devel. Genet.* **13**, 485 (1992).
15. R. K. Mortimer, D. Schild, C. R. Contopoulou, J. A. Kans, *Yeast* **5**, 321 (1989).
16. L. S. Symington, A. Brown, S. G. Oliver, P. Greenwell, T. D. Petes, *Genetics* **128**, 717 (1991).
17. N. P. Schultes and J. W. Szostak, *Mol. Cell. Biol.* **11**, 322 (1991); M. A. White, P. Detloff, M. Strand,

- T. D. Petes, *Curr. Genet.* **21**, 109 (1992).
18. D. S. Gross and W. T. Garrard, *Annu. Rev. Biochem.* **57**, 159 (1988).
19. L. W. Bergman and R. A. Kramer, *J. Biol. Chem.* **268**, 7223 (1983); A. Almer, H. Rudolph, A. Hirnen, W. Hörz, *EMBO J.* **5**, 2689 (1986); K. D. Fascher, J. Schmitz, W. Hörz, *J. Mol. Biol.* **231**, 658 (1993).
20. Y. Oshima, in *The Molecular Biology of the Yeast Saccharomyces: Metabolism and Gene Expression*, J. N. Strathern, E. W. Jones, J. R. Broach, Eds. (Cold Spring Harbor Laboratory, Cold Spring Harbor, NY, 1982), pp. 159-180.
21. S. G. Oliver *et al.*, *Nature* **357**, 38 (1992).
22. K. A. Nasmith, *Cell* **30**, 567 (1982); G. Thon and A. J. Klar, *Genetics* **131**, 287 (1992).
23. M. T. Berton and E. S. Vitetta, *J. Exp. Med.* **172**, 375 (1990).
24. M. T. Davison and T. H. Roderick, in *Genetic Variants and Strains of the Laboratory Mouse*, M. C. Green, Ed. (Fisher, Stuttgart, 1981), pp. 283-313; H. Donis-Keller *et al.*, *Cell* **51**, 319 (1987); B. J. Thomas and R. Rothstein, *ibid.* **64**, 1 (1991).
25. T.-C. Wu and M. Lichten, unpublished data.
26. DSB locations were determined by a comparison of DSB band positions in *rad50s* lanes [Fig. 2 and (25)] to positions of external standards (Hind III and Bst EII digests of bacteriophage  $\lambda$  DNA) and internal standards created by restriction enzyme digestion of mitotic yeast DNA. DSB frequencies were obtained with a combination of phosphorimage analysis (Fuji BAS2000) and video densitometry of autoradiograms (8). Dilutions of internal size standards were included in gels as concentration standards. Film density or fluorescent intensity values of these standards, of DSB bands, and of intact fragments were used to calculate DSB frequencies.
27. I. R. Beacham, B. W. Schweitzer, H. M. Warrick, J. Carbon, *Gene* **29**, 271 (1984); V. Rocco, M. J. Daly, V. Matre, M. Lichten, A. Nicolas, *Yeast* **9**, 1111 (1993); N. P. Schultes, personal communication.
28. Data contained in figure 3A of Symington *et al.* (16) were used to calculate crossover frequencies. Crossovers associated with gene conversion tracts with endpoints in two intervals were scored as half of a crossover in each interval.
29. Sporulation and direct DNA isolation from mitotic and meiotic cells were as described (8). Chromatin: spheroplasts were washed with spheroplasting buffer [P. T. Lowary and J. Widom, *Proc. Natl. Acad. Sci. U.S.A.* **86**, 8266 (1989)] plus protease inhibitors (10 mM sodium cacodylate, 2 mM iodoacetate, 0.2  $\mu$ M aprotinin, 130  $\mu$ M bestatin, 1  $\mu$ M leupeptin, 1  $\mu$ M pepstatin) and lysed in 100 mM sucrose, 10 mM tris-HCl (pH 7.5), 140 mM NaCl, 1 mM MgCl<sub>2</sub>, 0.2% NP-40, 0.5 mM phenylmethylsulfonyl fluoride, and protease inhibitor mix as above at 7.5% the original volume. Lysates were centrifuged 8 min at 6000g and pellets resuspended in digestion buffer [100 mM sucrose, 10 mM tris-HCl (pH 7.5), 140 mM NaCl, and 1 mM MgCl<sub>2</sub>] at 0.5% the original volume. DNA content was determined [C. F. Brunk, K. C. Jones, T. W. James, *Anal. Biochem.* **92**, 497 (1979)], and aliquots containing 15  $\mu$ g of DNA were digested at 0°C with DNase I for 1 min in 100  $\mu$ l of digestion buffer containing 2.5 mM CaCl<sub>2</sub> and 3.5 mM MgCl<sub>2</sub>. Digests were terminated in EDTA (12.5 mM), SDS (0.5%), and proteinase K (100  $\mu$ g/ml) for 2 hours at 65°C, and DNA was purified [R. H. Borts, M. Lichten, J. E. Haber, *Genetics* **113**, 551 (1986)]. Naked DNA controls were treated with DNase I in an identical manner. DNA samples were digested with restriction enzymes, displayed on agarose gels, transferred to nylon filters, and hybridized with radioactive probes. Restriction enzymes and probes were as follows. For *THR4* centromere-proximal and *LEU2-CEN3* regions, coordinates are from the chromosome III sequence (21). *ARG4* region (Fig. 2A): Nco I (cuts at -4.3 kb and +16.2 kb relative to the

*ARG4* translation start), and the probe is *Nco* I–*Bgl* II (–4.3 kb to –3.4 kb relative to *ARG4*). *THR4* centromere-proximal (Fig. 2B): *Bgl* II (nts 204996 to 215453), and the probe is *Hind* III–*Hind* III (nts 214047 to 214935). The band in lanes 1 and 17 through 23 of Fig. 2B apparently located just after the start of *YCR84w* is artifactual and is due to contamination of the probe with an adjacent fragment. *YCL14w-NFS1* (Fig. 2C): *Xho* I (nts 90286 to 99224), and the probe is *Kpn* I–*Eco* RI (nts 91185 to 91571). *YCL4w-YCL11c* (Fig. 2D): *Xho* I (nts 99224 to 118089), and the probe is *Eco* RI–*Hind* III (nts 100317 to 103054).

30. Diploid strains homozygous for *pho80ΔX::LEU2* or

*pho4Δ25::LEU2* (L. W. Bergman, personal communication) were constructed by transforming *leu2* derivatives of the haploid parents of NKY1002 with the appropriate deletion or disruption. Yeast DNA was extracted at the indicated time after induction of meiosis, digested with *Eco* RI (*Eco* RI cuts 2.6 kb upstream and >10 kb downstream of the *PHO5* translation start site), displayed on a 1.2% agarose gel, transferred to membranes, and hybridized with an *Eco* RI–*Cla* I fragment (–2.6 kb to –2.2 kb). DSB positions were determined with external standards (*Bst* EII digests of  $\lambda$  DNA) and internal standards comprising *Eco* RI/*Sal* I, *Eco* RI/*Bst* EII, and *Eco* RI and *Bam* HI double digests of DNA

from mitotic cells (*Sal* I, *Bst* EII, and *Bam* HI cut at nts +74, –185, and –542, respectively). DSB frequencies were determined as described above.

31. We thank L. Bergman, G. Simchen, N. Sugawara, and L. Symington for plasmids; M. Mendel and C. Wu for advice; G. Simchen, M. Smith, and C. Szent-Györgyi for prompting this study; L. Bergman, N. Schultes, and R. Malone for permission to cite unpublished data; and D. Chatteraj, C. Klee, J. Haber, A. Segall, R. Simpson, C. Vinson, M. Yarmolinsky, and C. Wu for comments that improved the manuscript.

10 August 1993; accepted 19 November 1993

## Effective Tumor Vaccine Generated by Fusion of Hepatoma Cells with Activated B Cells

Yajun Guo, Mengchao Wu, Hen Chen, Xiaoning Wang, Guanglu Liu, Guanglo Li, Jing Ma, Man-Sun Sy

Fusion of BERH-2 rat hepatocellular carcinoma cells with activated B cells produced hybrid cells that lost their tumorigenicity and became immunogenic. Syngeneic rats injected with BERH-2–B hybrid cells became resistant to challenge with parental BERH-2 cells, and rats with established BERH-2 hepatomas were cured by subsequent injection of BERH-2–B cells. Both CD4<sup>+</sup> and CD8<sup>+</sup> cells were essential for the induction of protective immunity; however, only CD8<sup>+</sup> cells were required for the eradication of BERH-2 tumors. The generation of hybrid tumor cells that elicit antitumor immune responses may be a useful strategy for cancer immunotherapy.

Tumor cells may escape immune surveillance because they do not express signals that are essential for activation of the host immune system (1, 2). At the molecular level, the defective signaling of tumor cells could be attributable to (i) down-regulation of major histocompatibility complex (MHC) molecules (3, 4); (ii) alteration of antigen-processing pathways, resulting in an inability to present tumor-specific antigens to host T cells (5); (iii) absence of costimulatory or adhesion molecules that are essential for activation of the host immune system (6); or (iv) production of factors that modify host immune responses (7).

Activated B cells are the most effective antigen-presenting cells (8). We hypothesized that fusion of a tumor cell with an activated B cell would produce a hybridoma that both expressed tumor-specific antigens and had the machinery for antigen presentation and T cell activation.

BERH-2 is a chemical carcinogen–induced hepatocarcinoma from the Wistar rat (9). Cells derived from this tumor grow rapidly and form tumors in the liver of syngeneic animals. We obtained activated B cells from the spleens of rats injected 14 days earlier with bovine serum albumin in Freund's complete adjuvant (10). BERH-2

cells were fused with purified activated B cells by treatment with polyethylene glycol (PEG) (11). The fused cells were enriched

by selection with a rabbit antiserum to BERH-2 cells and subsequent selection with a rabbit antiserum to rat B cells (10).

The parental BERH-2 cells expressed low amounts of MHC class I antigens and intracellular adhesion molecule–1 (ICAM-1) but were devoid of MHC class II antigens, leukocyte functional antigen–1 (LFA-1), and costimulatory molecule B7. In contrast, the BERH-2–B hybrid cell lines expressed MHC class II antigens, ICAM-1, LFA-1, and B7 (Fig. 1) and had enhanced expression of MHC class I antigens. These BERH-2–B cell lines have stably expressed both tumor and B cell antigens for more than 10 months.

All 10 rats injected intrahepatically with  $2 \times 10^6$  parental BERH-2 cells developed liver tumors and died within 60 days (12). In contrast, 10 rats injected with the same number of BERH-2–B hybrid cells remained tumor-free for 180 days (12). All four hybrid

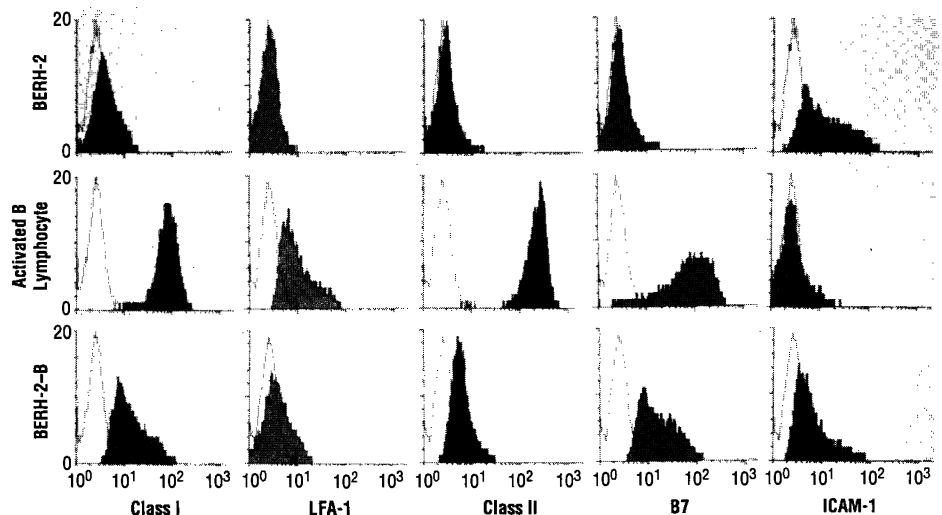


**Fig. 1.** Expression of MHC class I and class II antigens, B7, ICAM-1, and LFA-1 on BERH-2 cells, activated B cells, and BERH-2–B hybrid cells. Cells were washed with phosphate-buffered saline (PBS) and stained with monoclonal antibodies to rat MHC class I (OX-18), MHC class II (OX-6), ICAM-1 (IA 29), or LFA-1 (WT.1). To stain for rat B7, we used CTLA4-Ig, a soluble fusion protein containing the variable domain of the human CTLA-4 protein and the hinge, CH2, and CH3 domains of the human IgG1 constant region (14). Cells were incubated with the antibodies or chimeric protein for 30 min on ice. A mouse antibody to human CD3 (GH3, IgG2b) and a soluble human CD44-Ig chimeric protein were used as negative controls. Cells were washed three times. Fluorescein isothiocyanate (FITC)–conjugated goat antibody to mouse Ig or FITC-labeled rabbit antibody to human Ig was added for another 30 min on ice. Samples were then washed, fixed, and analyzed in a FACScan (Becton Dickinson, San Jose, California). Solid areas are cells stained with specific antibodies. Open areas are cells stained with control antibodies.

Y. Guo, M. Wu, H. Chen, X. Wang, G. Liu, G. Li, Tumor Immunology and Biotherapy Center, Eastern Institute of Hepatobiliary Surgery, Shanghai 200433, China. Y. Guo, J. Ma, M.-S. Sy, Institute of Pathology, Case Western Reserve University, Cleveland, OH 44106.